Propagation, Stability and Instability of Large Amplitude Internal Waves

Bruce Sutherland

Depts. of Physics and of Earth & Atmospheric Sciences
University of Alberta

February 3, 2013

Solitary Waves

- solitary waves in the atmosphere and ocean
- Korteweg de Vries equations and extension to radially spreading waves
- shoaling solitary waves

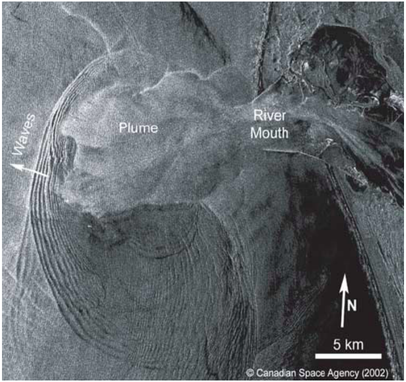

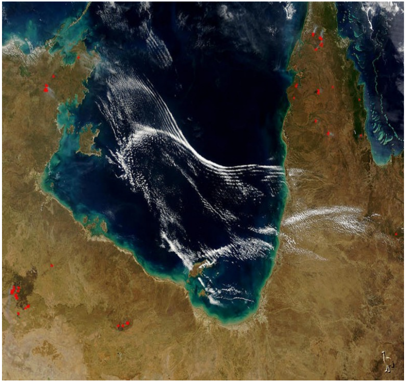

Solitary Waves in the Ocean and Atmosphere

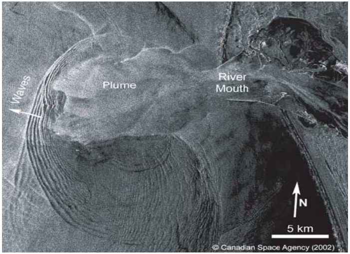

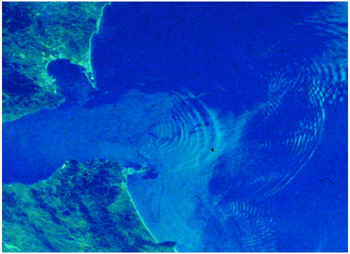

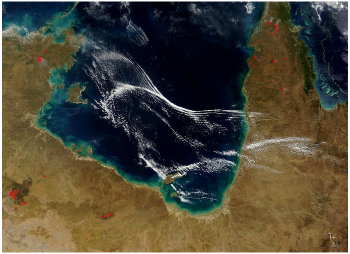

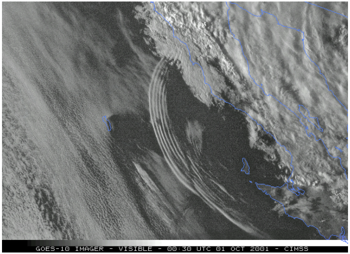

River Plumes

Columbia River

- A plume of freshwater propagates along the surface of a salt-stratified ambient.
- Surface waters are displaced downwards, forming a large amplitude wave.
- Wave separation occurs when the plume decelerates.

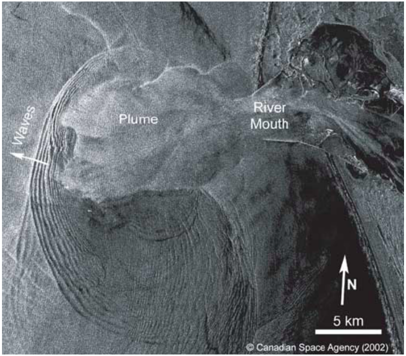

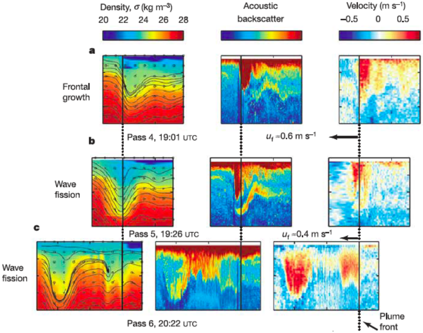

[Nash & Moum, Nature (2005)]

Atmospheric Gravity Currents

- Thunderstorm outflows, the collision of storm fronts, etc create gravity currents that can go on to excite solitary waves in the atmosphere

Morning Glory east of Burketown, 1996

[from http://www.dropbears.com/brough/]

Undular Bore west of Baja Peninsula

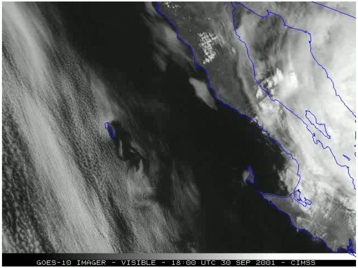

Generating Solitary Waves from Gravity Currents

- Thunderstorm outflows are blasts of cold air that flow under an atmospheric inversion.

- This is modelled in the laboratory with dense fluid moving in a shallow layer of a 2-layer fluid.

Surface Solitary Waves

- Korteweg-de Vries (KdV) solitary waves result from balance of nonlinear steepening and (linear) wave dispersion
- Their evolution is governed by Korteweg-de Vries equation:

$$\eta_t + c_0\eta_x + \frac{3c_0}{2H}\eta\eta_x + \frac{1}{6}c_0 H^2 \eta_{xxx} = 0$$

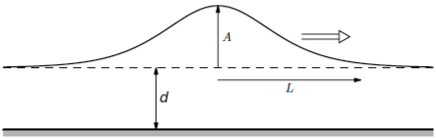

$$\eta(x,t) = A\,\mathrm{sech}^2\left(\frac{x-ct}{\lambda}\right)$$

Width: $\lambda = \sqrt{\frac{4H^3}{3A}}$

Speed: $c = c_0\left(1 + \frac{1}{2}\frac{A}{H}\right)$

Solitary Waves in Stratified Fluids

- Atmospheric and oceanic solitary waves exist in continuously stratified fluid.
- For example, they can be generated by lock-release experiments in uniformly stratified fluid.

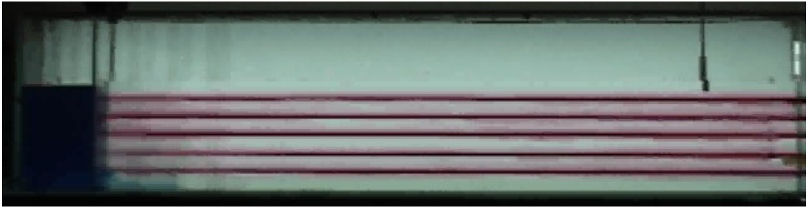

[Munroe et al, J. Fluid Mech. (2009)]

Derivation of Internal KdV Equation

- Start with the governing 2D hydrostatic, Boussinesq equations:

$$\begin{aligned}
\rho_0 u_t + p_x &= -\rho_0(u u_x + w u_z) \\
p_z + \rho g &= 0 \\
\rho_t + w\bar{\rho}' &= -(u\rho_x + w\rho_z) \\
u_x + w_z &= 0
\end{aligned}$$

  and relate these to the vertical displacement field using $w = D\xi/Dt$:

$$w - \xi_t \simeq u\xi_x$$

- Expand the fields in terms of the amplitude parameter, α:

$$\xi(x,z,t) = \alpha\xi_0 + \alpha^2\xi_1 + \ldots$$

- Assume

$$\xi_0 = \eta(x,t)\,\phi(z) \quad \text{with} \quad \eta \equiv A(\epsilon(x - c_0 t), \epsilon\alpha t)$$

  - $\phi(z)$ is vertical structure and c_0 the shallow water speed given by linear theory

Internal Solitary Waves

Rectilinear Theory

- Assume $\epsilon \simeq \alpha$ and keep terms to order α^3.
- The result is the KdV equation for the maximum deflection:

$$\eta_t + c_0\eta_x + \gamma\eta\eta_x + \beta\eta_{xxx} = 0$$

$$\gamma = \frac{3}{2}c_0\frac{\int \bar{\rho}\phi_z^3\,dz}{\int \bar{\rho}\phi_z^2\,dz} \qquad \text{and} \qquad \beta = \frac{1}{2}c_0\frac{\int \bar{\rho}\phi^2\,dz}{\int \bar{\rho}\phi_z^2\,dz}$$

Solution:

$$\boxed{\begin{array}{l} \eta(x,t) = A\,\mathrm{sech}^2\left(\dfrac{x-ct}{\lambda}\right) \\ \text{Width: } \lambda = \sqrt{\frac{12\beta}{\gamma}\frac{1}{A}} \\ \text{Speed: } c = c_0 + \frac{\gamma}{3}A \end{array}}$$

Note: Results are consistent with a surface solitary wave.

Non-KdV Solitary Waves

- If the solitary wave is forced at very large amplitude, its crest flattens and the wave broadens.

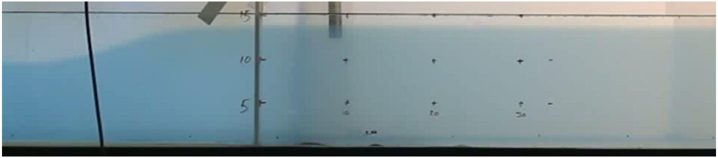

  - several “modified” KdV equations have been proposed to capture this structure.
- Extremely large solitary waves exhibit breaking and/or closed cores.

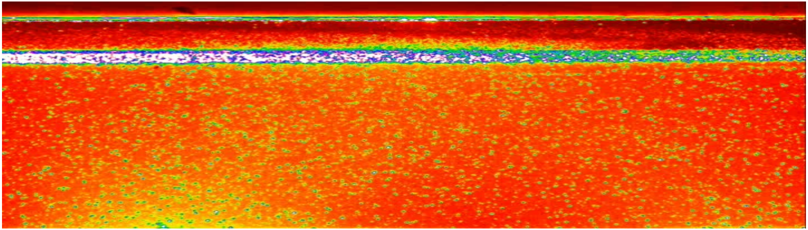

[Magda Carr, http://www-vortex.mcs.st-and.ac.uk/˜ magda/research.html]

  - Dubreuil-Jacotin-Long equation sometimes used to describe these waves

Radially Spreading Solitary Waves

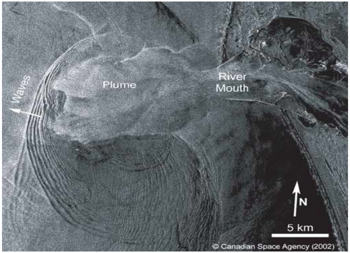

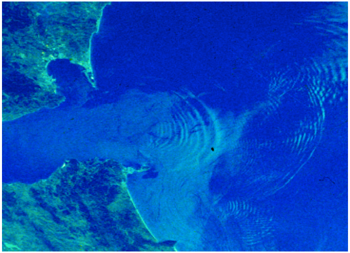

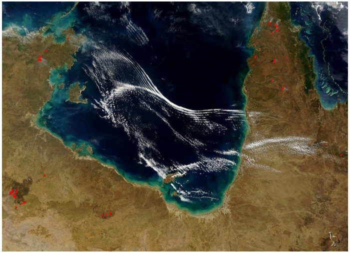

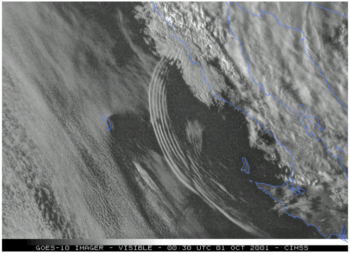

In all these images wave fronts spread radially from a localized source.

Radial Intrusions at a Thick Interface

- Intrusion should slow down as it spreads, but it does not!

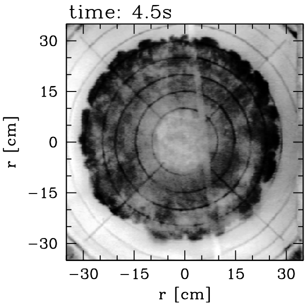

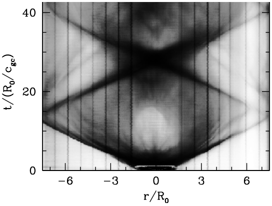

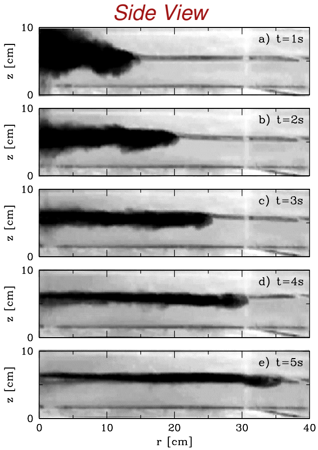

Numerical Simulations

Initialization:

- specify the initial density field – hyperbolic tangent profile
- use experimental parameters for densities and depths
- vary interface thickness and tank radius
- include a passive tracer to simulate dyed lock fluid

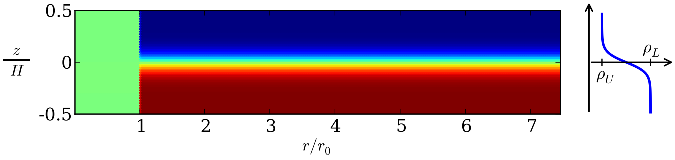

Results:

Vertical velocity field

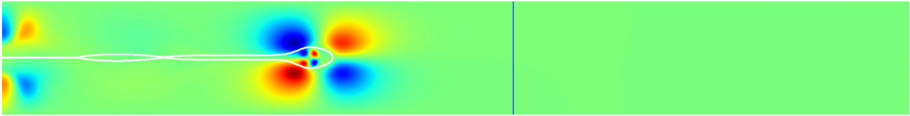

[McMillan & BRS, Nonlin. Proc. Geophys. (2010)]

"Rigorous" Derivation of Axisymmetric KdV Equation

- Start with the governing axisymmetric equations:

$$\rho_0 u_t + p_r = -\rho_0(uu_r + wu_z)$$
$$p_z + \rho g = 0$$
$$\rho_t + w\bar{\rho}\,' = -(u\rho_r + w\rho_z)$$
$$\frac{1}{r}(ru)_r + w_z = 0$$
$$w - \xi_t \simeq \frac{1}{r}(r\xi u)_r$$

- Expand the fields in terms of the amplitude parameter, α:

$$\xi(r,z,t) = \alpha\xi_0 + \alpha^2\xi_1 + \ldots$$

- Assume

$$\xi_0 = \eta(r,t)\,\phi(z) \quad \text{with} \quad \eta \equiv \left(\frac{r}{r_0}\right)^{-1/2} A(\epsilon(r - c_0 t), \epsilon\alpha t)$$

Here $\phi(z)$ is the vertical structure given by linear theory.

Axisymmetric KdV Equation Result

- Assume $r \gg r_0$ and extract terms up to $O(\alpha^2)$:

$$\eta_t + c_0 \left(\eta_r + \frac{\eta}{2r} \right) + \gamma \eta \eta_r + \beta \eta_{rrr} = 0$$

- Consistent with axisymmetric surface solitary wave eqn [Miles, JFM (1978)]
- But result is asymptotically inconsistent [Weidman and Zakhem, JFM (1988)]
  - derivation requires $r \gg r_0$
  - but nonlinearity becomes negligible at large r

Axisymmetric KdV Equation Result

- Assume $r \gg r_0$ and extract terms up to $O(\alpha^2)$:

$$\eta_t + c_0\left(\eta_r + \frac{\eta}{2r}\right) + \gamma\eta\eta_r + \beta\eta_{rrr} = 0$$

- Consistent with axisymmetric surface solitary wave eqn [Miles, JFM (1978)]
- But result is asymptotically inconsistent [Weidman and Zakhem, JFM (1988)]
  - derivation requires $r \gg r_0$
  - but nonlinearity becomes negligible at large r
- The equation also differs from the equation assuming a KdV structure:

$$\eta_t + c_0\left(\eta_r + \frac{\eta}{2r}\right) + \gamma\left(\frac{r}{r_0}\right)^{1/2}\eta\eta_r + \beta\eta_{rrr} = 0$$

with solution $\eta \propto \text{sech}^2\left(\frac{r-ct}{\lambda}\right)/\sqrt{r}$, as seen in simulations.

- More theoretical work needs to be done . . .

Shoaling Solitary Waves in the South China Sea

- Internal waves are launched by tides flowing through the Luzon Strait.
- Eventually these steepen to form internal solitary waves (large-amplitude undulations of the thermocline).
- Where the waves break they can resuspend sediments (and nutrients) enhancing, for example, the development of the coral reef at Dongsha.

Bathymetry of the South China Sea

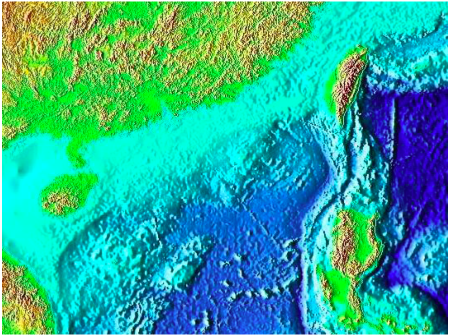

Internal Solitary Waves Approaching Dongsha

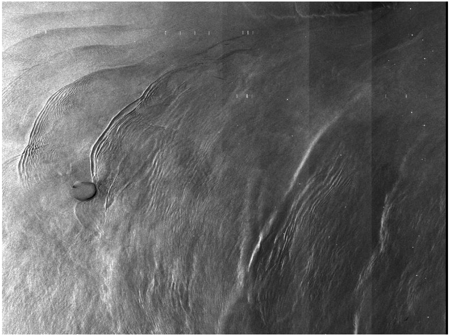

Internal Solitary Wave Generation and Shoaling

- A series of experiments were performed in which internal solitary waves, generated by lock-release, propagated toward a slope.

Internal Solitary Wave Generation and Shoaling

- A series of experiments were performed in which internal solitary waves, generated by lock-release, propagated toward a slope.

- How the waves shoal on a slope is assessed by the Iribarren Number:

$$\text{Ir} = \frac{\text{topographic slope}}{\text{wave slope}} = \frac{s}{A/L}$$

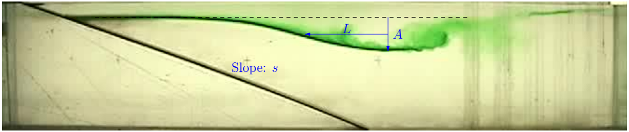

Shallow and Steep Slopes

Tumbling breaker: $\mathit{Ir} = 0.69$

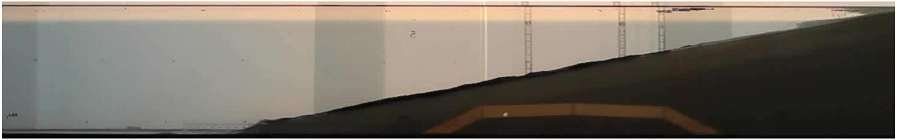

Spilling breaker: $\mathit{Ir} = 1.34$

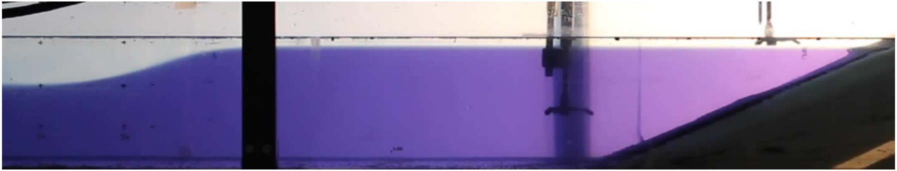

Resuspension from Shoaling Solitary Waves

- When an internal wave encounters a slope, sediment is carried downslope in advance of the wave.
- Particles may resuspend where the trailing edge of the wave reaches the slope.

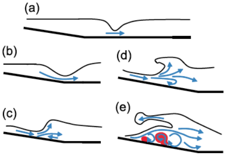

[Boegman & Ivey, JGR (2009)]

Solitary Wave Maximum Descent

- When solitary wave shoals, assume its area wave fills a triangle of height $h_\star$ and length $l_\star = h_\star/s$.
- Equate this area with the area, $A_{sw}(2L_{sw})$, of the incident internal solitary wave:

$$2A_{sw}L_{sw} = \frac{1}{2}h_\star l_\star = \frac{1}{2s}{h_\star}^2$$

- So expect maximum deepening is

$$h_\star \simeq \sqrt{4sA_{sw}L_{sw}}.$$

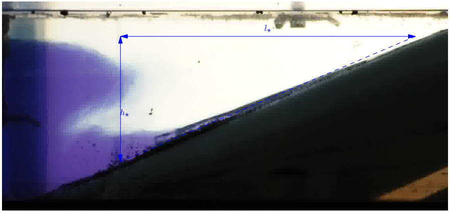

Solitary Wave Maximum Descent

- When solitary wave shoals, assume its area wave fills a triangle of height $h_\star$ and length $l_\star = h_\star/s$.
- Equate this area with the area, $A_{sw}(2L_{sw})$, of the incident internal solitary wave:

$$2A_{sw}L_{sw} = \frac{1}{2}h_\star l_\star = \frac{1}{2s}{h_\star}^2$$

- So expect maximum deepening is

$$h_\star \simeq \sqrt{4sA_{sw}L_{sw}}.$$

- This is consistent with experiments.

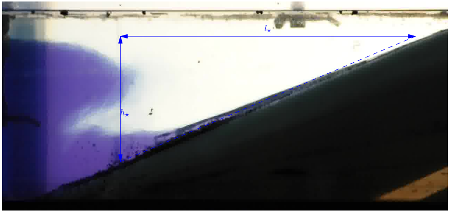

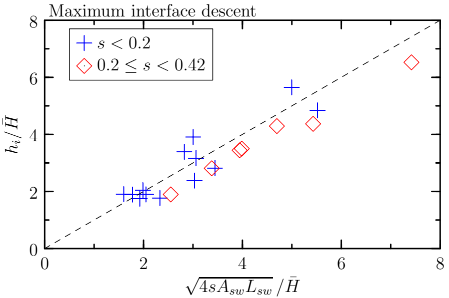

Sediment Transport and Resuspension

- The ADCPs measure the along slope speeds u_s, 0.5 cm above the bottom of the slope.
- The maximum downslope speed above the maximum descent scales approximately with the incoming solitary wave speed.

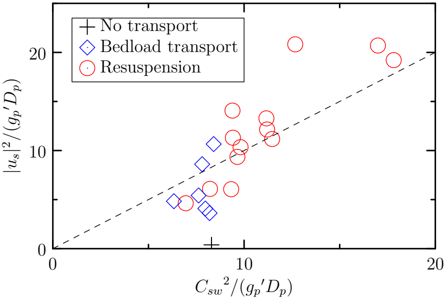

Sediment Transport and Resuspension

UNIVERSITY OF ALBERTA

- The ADCPs measure the along slope speeds u_s, 0.5 cm above the bottom of the slope.
- The maximum downslope speed above the maximum descent scales approximately with the incoming solitary wave speed.

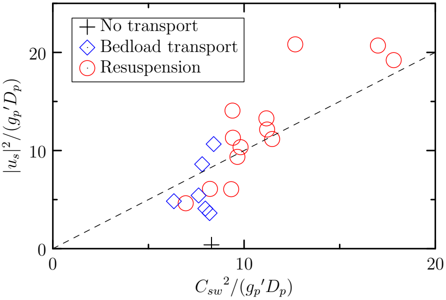

- Define the Shield's parameter to be the ratio of bottom stress to the buoyancy of the particles (with reduced gravity $g_p{}'$ and diameter d_p):

$$\text{Sh} \equiv \frac{{u_s}^2}{g_p{}' d_p}$$

  - along-slope transport if $\text{Sh} \gtrsim 1$
  - resuspension at maximum depth if $\text{Sh} \gtrsim 5$

Limitations of the Shields Parameter

- The Shields parameter comes from studying bedform deformations in river flows.
- It assumes steady, uniform density flow and predicts transport and resuspension as the flow speed increases.
- However, internal solitary waves resuspend sediment at the separation point, where the flow speed (hence Sh) goes to zero.
- A new diagnostic should be created to predict resuspension in transient stratified flows.

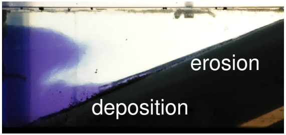

Modulational Stability/Instability

- derivation of stability condition
- nonlinear Schrödinger equation
- modulational stability and instability of internal waves

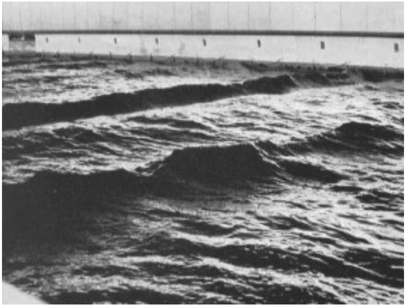

Modulational Stability (Part 1)

- For $\eta(x,t) = Ae^{\imath\theta}$, define $\omega \equiv -\theta_t$; $k \equiv \theta_x \Rightarrow \frac{\partial k}{\partial t} + \frac{\partial \omega}{\partial x} = 0$
- Energy conservation requires $\frac{\partial}{\partial t}(f(k)A^2) + \frac{\partial}{\partial x}(c_g f(k)A^2) = 0$
  - $f(k)$ is function set so that fA^2 is energy
- Suppose weakly nonlinear dispersion relation is $\omega = \omega_0(k) + \omega_2(k)A^2$
  - conservation laws become

$$\frac{\partial k}{\partial t} + \left[{\omega_0}' + \omega_2' A^2\right] \frac{\partial k}{\partial x} + \omega_2 \frac{\partial A^2}{\partial x} = 0$$

$$f' \frac{\partial k}{\partial t} A^2 + f \frac{\partial A^2}{\partial t} + f' \frac{\partial k}{\partial x} c_g A^2 + f {c_g}' \frac{\partial k}{\partial x} A^2 + f c_g \frac{\partial A^2}{\partial x} = 0$$

- Simplify to get matrix equation

$$\begin{pmatrix} \frac{\partial k}{\partial t} \\ \frac{\partial A^2}{\partial t} \end{pmatrix} + \begin{bmatrix} {\omega_0}' & \omega_2 \\ {\omega_0}'' A^2 & {\omega_0}' \end{bmatrix} \begin{pmatrix} \frac{\partial k}{\partial x} \\ \frac{\partial A^2}{\partial x} \end{pmatrix} = 0$$

Modulational Stability (Part 2)

- Matrix equation is advection equation: $\frac{\partial \underline{u}}{\partial t} + \mathbf{C}\frac{\partial \underline{u}}{\partial x} = 0$

  with $\underline{u} \equiv \left(\begin{array}{c} k \\ A^2 \end{array}\right)$ and $\mathbf{C} \equiv \left[\begin{array}{cc} {\omega_0}' & \omega_2 \\ {\omega_0}'' A^2 & {\omega_0}' \end{array}\right]$
- Eigenvalues of $\mathbf{C}$ are $\lambda \,(= \frac{dx}{dt}) = {\omega_0}' \pm A\,[\omega_2\,{\omega_0}'']^{1/2}$
- Case 1: $\omega_2\,{\omega_0}'' > 0$.
  - Initial disturbance splits into two separate wavepackets moving at speeds greater and less than c_g.
  - such wavepackets are *modulationally stable*
- Case 2: $\omega_2\,{\omega_0}'' < 0$.
  - Initial disturbance grows exponentially at rate $\propto A$.
  - such wavepackets are *modulationally unstable*

Modulational Instability of Deep Water Waves

- For moderately large deep water waves, the dispersion relation is

$$\omega = \sqrt{gk}\left(1 + \frac{1}{2}k^2 A^2\right).$$

  - So $\omega_2 = \frac{1}{2}\sqrt{gk}\,k^2$ and $\omega_0'' = -\frac{1}{4}\sqrt{\frac{g}{k^3}}$
- Hence $\omega_2\,\omega_0'' = -gk/8 < 0$: deep water waves are always unstable!

Periodic waves near source

Disintegrated wave train downstream

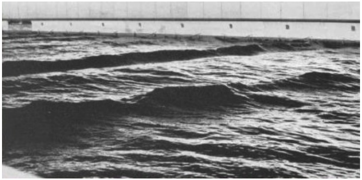

Modulational Instability of Deep Water Waves

UNIVERSITY OF ALBERTA

- For moderately large deep water waves, the dispersion relation is

$$\omega = \sqrt{gk}\left(1 + \frac{1}{2}k^2 A^2\right).$$

  - So $\omega_2 = \frac{1}{2}\sqrt{gk}\,k^2$ and $\omega_0'' = -\frac{1}{4}\sqrt{\frac{g}{k^3}}$
- Hence $\omega_2\,\omega_0'' = -gk/8 < 0$: deep water waves are always unstable!

Periodic waves near source

Disintegrated wave train downstream

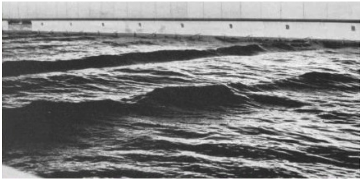

- Generally, all "non-shallow" interfacial internal waves are modulationally unstable, with marginal stability as $k\bar{H} \to 0$.

The Nonlinear Schrödinger Equation

- For finite amplitude waves, suppose dispersion relation is

$$\omega(k,|A|^2) \simeq \omega|_{(k_0,0)} + \left.\frac{\partial\omega}{\partial k}\right|_{(k_0,0)}(k-k_0) + \frac{1}{2}\left.\frac{\partial^2\omega}{\partial k^2}\right|_{(k_0,0)}(k-k_0)^2 + \left.\frac{\partial\omega}{\partial|A|^2}\right|_{(k_0,0)}|A|^2$$

- Solving as before . . . $\imath(A_t+\omega'(k_0)A_x)+\frac{1}{2}\omega''(k_0)A_{xx}-\omega_2|A|^2A=0$, where $\omega_2=\left.\frac{\partial\omega}{\partial|A|^2}\right|_{|A|^2=0}$

- In translating frame, $X=x-c_gt$, gives the *Nonlinear Schrödinger Equation*:

$$A_t=\imath\frac{1}{2}\omega''(k_0)A_{XX}-\imath\omega_2|A|^2A$$

The Nonlinear Schrödinger Equation

- For finite amplitude waves, suppose dispersion relation is

$$\omega(k,|A|^2) \simeq \omega|_{(k_0,0)} + \left.\frac{\partial\omega}{\partial k}\right|_{(k_0,0)}(k-k_0) + \frac{1}{2}\left.\frac{\partial^2\omega}{\partial k^2}\right|_{(k_0,0)}(k-k_0)^2 + \left.\frac{\partial\omega}{\partial|A|^2}\right|_{(k_0,0)}|A|^2$$

- Solving as before ... $\imath(A_t + \omega'(k_0)A_x) + \frac{1}{2}\omega''(k_0)A_{xx} - \omega_2|A|^2 A = 0$,
  where $\omega_2 = \left.\frac{\partial\omega}{\partial|A|^2}\right|_{|A|^2=0}$

- In translating frame, $X = x - c_g t$, gives the *Nonlinear Schrödinger Equation*:

$$A_t = \imath\frac{1}{2}\omega''(k_0)A_{XX} - \imath\omega_2|A|^2 A$$

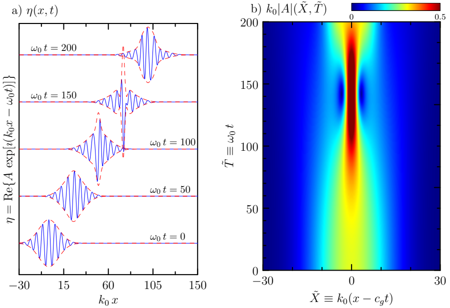

The Boussinesq NLS Equation for Internal Waves

- Assume the leading order weakly nonlinear dynamics for internal waves results from the wave-induced mean flow Doppler shifting the waves:

$$\partial_t A + c_{gz}\partial_z A = \imath \frac{1}{2}\omega_{mm}\partial_{zz}A - \imath k U A$$

in which $U = -\langle \xi\zeta \rangle \propto |A|^2$

- Compare with generic form of the NLS equation:

$$A_t = \imath \frac{1}{2}\omega'' A_{XX} - \imath\omega_2 |A|^2 A$$

- For Boussinesq internal waves, $\omega_2 > 0$. So, according to the criterion for modulational stability, which depends upon the sign of $\omega_2\,\omega_0{}''$, moderately large wavepackets are ...
  - unstable if $N > \omega > \sqrt{\frac{2}{3}} \simeq 0.82\,N$ $\quad$ ($|m| < \frac{1}{\sqrt{2}}\,|k| \simeq 0.71\,|k|$)
  - stable if $\omega < \sqrt{\frac{2}{3}}N \simeq 0.82\,N$ $\quad$ ($|m| > \frac{1}{\sqrt{2}}\,|k| \simeq 0.71\,|k|$)

Moderately Large Internal Waves

Wavepackets with amplitude $A \equiv A_\xi / \lambda_x = 0.048$

$\underbrace{k_z = -0.4\,k_x, (\Theta \simeq 22^o)}$ $\underbrace{k_z = -1.4\,k_x, (\Theta \simeq 55^o)}$

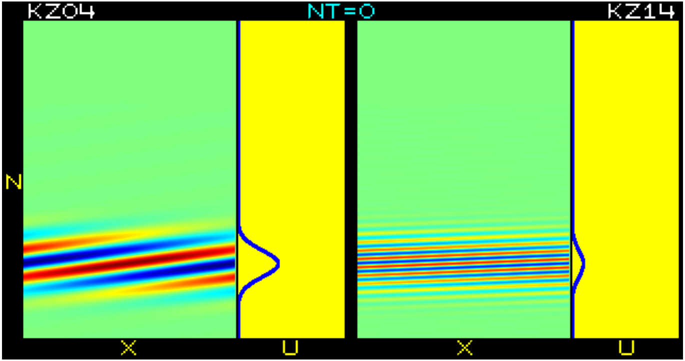

contours: $|\xi| \leq 0.048\,\lambda_x$ U range: $0 \leq \langle U \rangle \leq c_{gx}$

[BRS, J. Fluid Mech. (2006)]

Wave Generation by Turbulence

- generation by flow over rough topography
- generation by oscillatory turbulent patch
- generation by convective storms

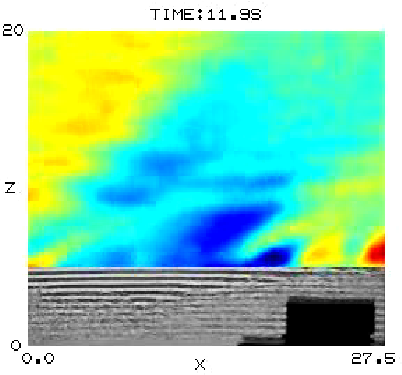

Flow Rough Terrain and Turbulence

- Internal waves are generated in the lee of fast flow over rough terrain.
- At late times, quasi-monochromatic waves appear above the turbulent wake.

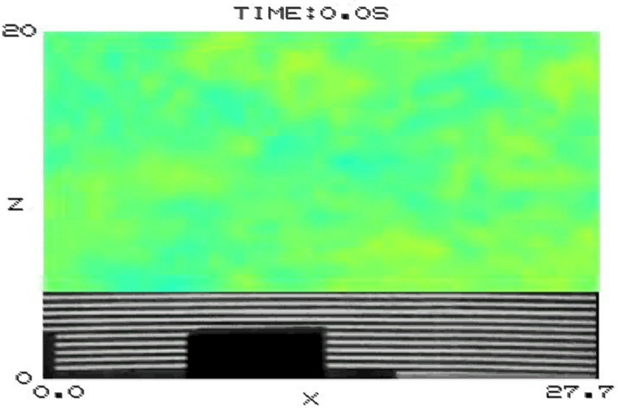

[Aguilar & BRS, Phys. Fluids (2006)]

Also see simulations by Diamessis et al, J. Comp. Phys. (2005)

Breaking Internal Waves

Internal Wave Generation, Propagation and Breaking

[Clark & BRS, Phys. Fluids (2010)]

Internal Wave Generation by Storms

- Internal waves originate from a storm in the troposphere.
- They propagate through the middle atmosphere and are visualized by OH airglow in ionosphere.

[Movie by Dave Sentman, U. Alaska. Taken from Black Hills, SD looking ESE toward a storm over Nebraska, August 18 1999.]

Generation by Storms

Experimental Setup

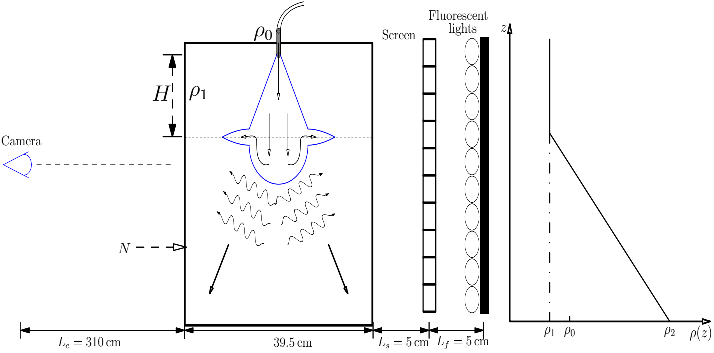

- Laboratory experiments model the mechanical oscillations of a storm near the tropopause as a plume impacting stratified fluid.
- In the laboratory it is convenient to set-up the experiments “upside-down”
  - inject salty fluid downward in uniform-density fresh water (the model troposphere)
  - waves are generated in the underlying uniformly stratified fluid (the model stratosphere)

Generation by Storms

Composite movie from experiment

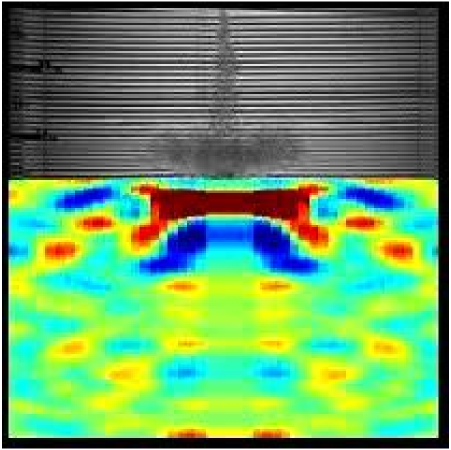

[Ansong & BRS, J. Fluid Mech. (2010)]

Internal Wave Breaking

- gravity wave drag parameterization
- breaking at critical levels, the quasi-biennial oscillation
- anelastic growth and breaking

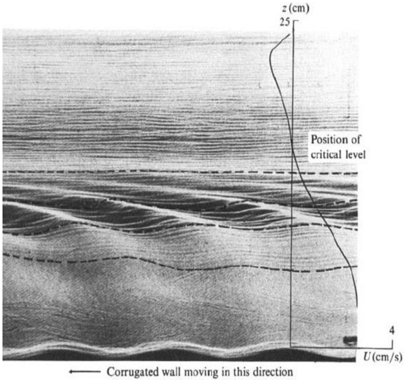

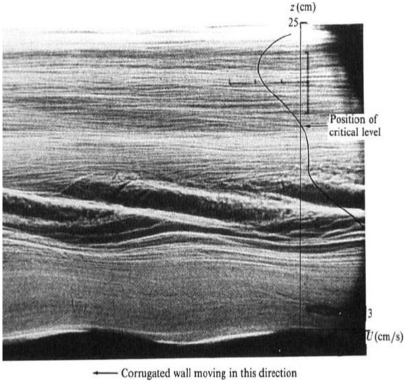

GCMs without Internal Waves

- Small spatial-scale, fast time-scale internal wave dynamics are not captured by general circulation models (GCMs) of the atmosphere.
- But without internal waves, observed mean winds and temperature are not well reproduced. In particular . . .
  - the winter-hemisphere Jet Stream does not peak at the tropopause (it is not “closed”)
  - wind speeds are too strong at high altitudes

Observed Zonal Winds

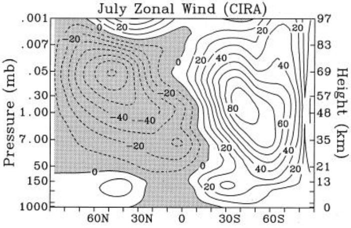

From Figure 10a of McLandress (1998)

Simulated Winds with Insufficient Drag

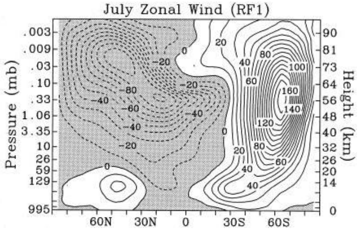

From Figure 10b of McLandress (1998)

A Simple View of Momentum Transport and Deposition

UNIVERSITY OF ALBERTA

- We may combine the concept of critical levels and anelastic growth to predict heuristically where internal waves deposit their momentum in the atmosphere:
  - waves deposit their momentum at a critical level (where their horizontal phase speed matches the background flow speed)

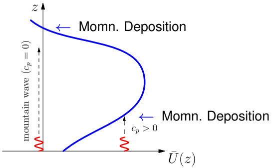

  - waves grow anelastically until they reach their overturning amplitude and then continually deposit momentum to the mean flow so they remain at that amplitude

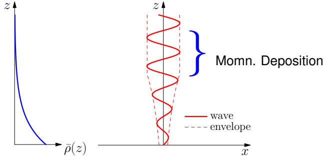

- This was first proposed by *Lindzen (1981)* as an efficient method to include momentum transport by internal waves in coarse-resolution general circulation models.

Internal Wave Breaking: Critical Level in Ambient Shear

- Upward propagating internal waves break and exert drag near a critical level.
- Large amplitude or sustained wave breaking can change the mean flow itself. In this way the height of the critical level descends.

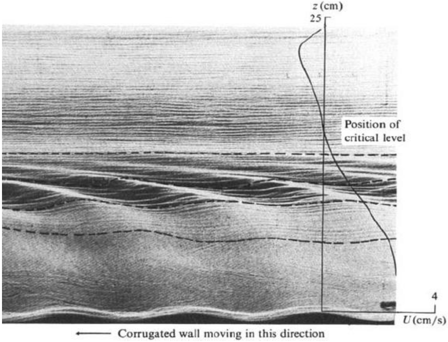

[From Figure 5 of Koop and McGee, J. Fluid Mech (1986)]

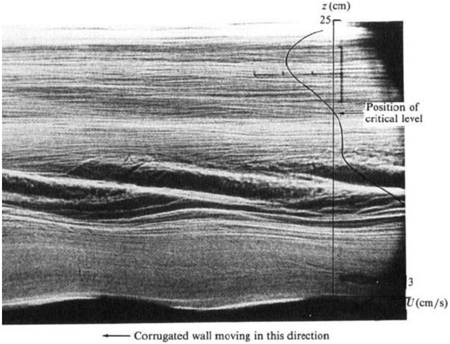

[From Figure 7 of Koop and McGee, J. Fluid Mech (1986)]

The Quasi-Bienniel Oscillation

UNIVERSITY OF ALBERTA

- Beginning in the mid 1950s, observations showed that the stratospheric tropical winds (between 20-30 km) flowed alternately eastward and westward.
- Typically winds with zero velocity descended over time on a two-year cycle.
- Eventually this behaviour was attributed to breaking waves alternately depositing momentum eastward and westward.
- Though originally thought to be Kelvin and Rossby waves, it is now believed internal waves dominately drive the mean flow.

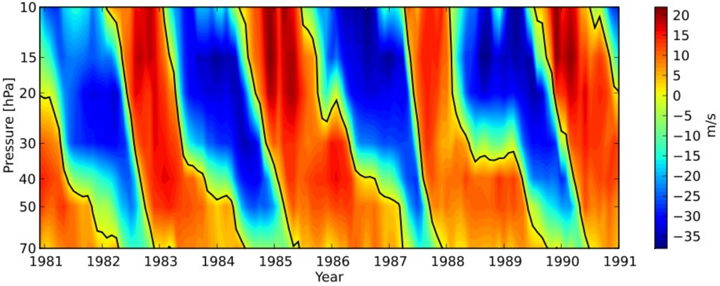

Theory for the Quasi-Bienniel Oscillation

- Waves propagate upward with eastward and westward phase speeds.
- These are alternately absorbed by winds in the stratosphere which changes the wind speed.

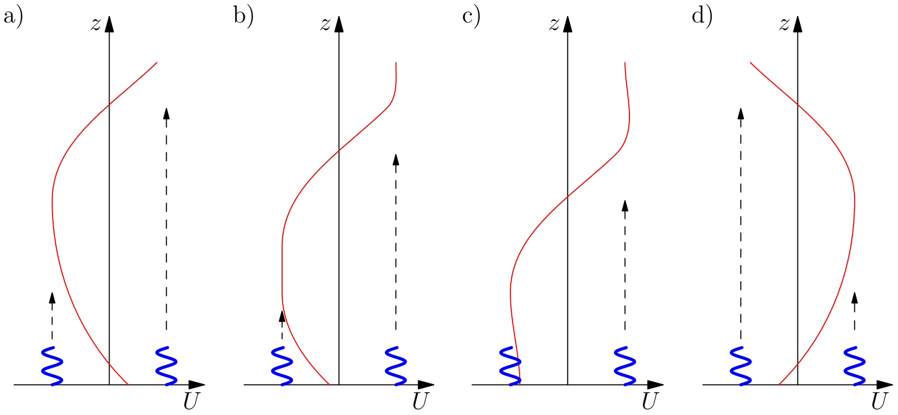

A Laboratory Model of the Quasi-Bienniel Oscillation

UNIVERSITY OF ALBERTA

- An annular tank ($R_o = 0.30\,\text{m}$, $R_i = 0.18\,\text{m}$) is filled $0.44\,\text{m}$ deep with salt-stratified fluid having buoyancy frequency $N = 1.6\,\text{s}^{-1}$.
- 16 pads at bottom alternately move up and down at fixed frequency and amplitude.
- These launch a superposition of left- and right-moving waves

Side View

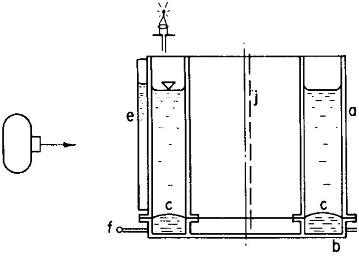

Top View

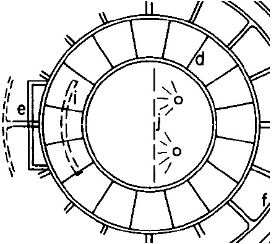

McEwan and Plumb, J. Atmos. Sci. (1977)

A Laboratory Model of the Quasi-Bienniel Oscillation

- After a few hours, the system settles into a steady state in which the standing waves (a superposition of leftward and rightward waves) alternately deposit momentum leftward and rightward where they encounter a descending critical level.
- Where the waves break, they deposit momentum in the direction of the flow at that level and the position of the critical level descends.

[From experiments by McEwan & Plumb (1977)]
Frequency: $\omega = 0.43\,\mathrm{s}^{-1}$ Amplitude: $A = 0.8$ mm
The movie is sped up 100 times.

- Embedded particles visualize the alternately leftward and rightward moving flow that descends in time.

Wave Breaking through Anelastic Growth

- Due to momentum conservation, the amplitude of internal waves must increase as they move upwards into less dense fluid. This is referred to as *anelastic growth*.

- The mean density, $\bar{\rho}(z)$, of the atmosphere decreases at an approximately exponential rate. So atmospheric internal waves grow exponentially in height (though with twice the density's e-folding height).
  - For example, the density at the tropopause is about 1/4 that at sea level. So waves will double in amplitude going upward through the troposphere.
  - Likewise their amplitude increases tenfold going through the stratosphere.

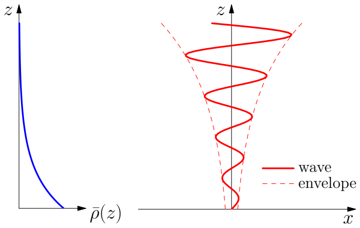

- Eventually, the amplitude of internal waves becomes so large that they break and deposit their momentum to the background flow.

Anelastic Growth of a Wavepacket in Linear Theory

- A horizontally periodic, vertically localized wavepacket grows exponentially in height as it advances upward.

- The waves are predicted to overturn at

$$z_b = 2H_\rho \ln\left(\frac{1}{|m\,A_{\xi 0}|}\right).$$

where m is the vertical wavenumber and $A_{\xi 0}$ is the initial maximum vertical displacement at $z = 0$.

- In a simulation that neglects the nonlinear advective terms, $\vec{u}\cdot\nabla(\cdot)$, the waves continue to grow exponentially even after they are overturning.
- In reality, we anticipate they should break above the overturning level.

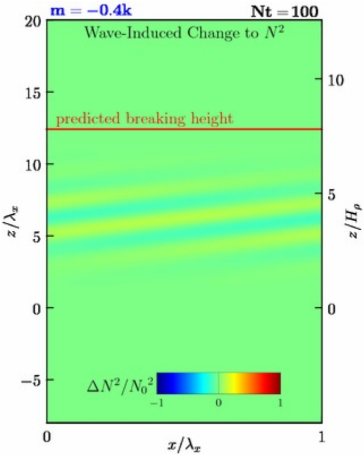

A Modulationally Unstable Anelastic Wavepacket

- Wavepackets with $|m| < |k|/\sqrt{2} \sim 0.71|k|$ are modulationally unstable.
- The interaction becomes more significant as the waves grow in amplitude
- Eventually this changes the wave structure: the packet narrows and increases in amplitude
- This leads to overturning below the level predicted by linear theory

Simulation initialized with wavepacket: $\xi = A_{\xi 0}\, e^{-z^2/2\sigma^2} \left(e^{\imath(kx+mz-\omega t)} e^{z/2H_\rho}\right)$

$$m = -0.4k, \quad A_{\xi 0} \simeq 0.008\lambda_x, \quad \sigma = H_\rho \simeq 1.6\lambda_x$$

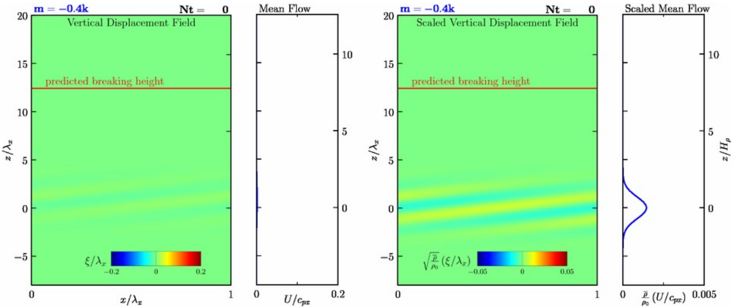

[Dosser & BRS, J. Atmos. Sci (2011)]

A Modulationally Stable Anelastic Wavepacket

- Wavepackets with $|m| > |k|/\sqrt{2} \sim 0.71|k|$ are modulationally stable.
- Such packets broaden and decrease in amplitude
- This leads to overturning above the level predicted by linear theory

Simulation initialized with wavepacket: $\xi = A_{\xi 0}\, e^{-z^2/2\sigma^2} \left(e^{\imath(kx+mz-\omega t)} e^{z/2H_\rho} \right)$

$$m = -1.4k, \quad A_{\xi 0} \simeq 0.008\lambda_x, \quad \sigma = H_\rho \simeq 1.6\lambda_x$$

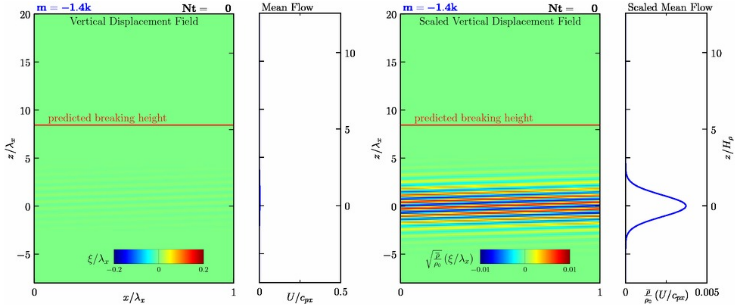

[Dosser & BRS, J. Atmos. Sci (2011)]

Simulated Overturning Heights

- For strongly non-hydrostatic waves with $|m| \lesssim |k|/\sqrt{2} \simeq 0.71|k|$ waves break below the level predicted by linear theory. Breaking occurs well below if $Hk \gg 1$.
- For more hydrostatic waves with $|m| \gtrsim |k|/\sqrt{2}$ waves break above the level predicted by linear theory. Breaking occurs well above if $|m/k|$ is large.

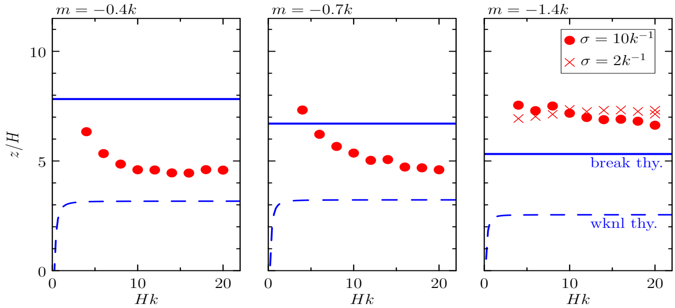

[Dosser & BRS, J. Atmos. Sci (2011)]

Simulated Overturning Heights

- For strongly non-hydrostatic waves with $|m| \lesssim |k|/\sqrt{2} \simeq 0.71|k|$ waves break below the level predicted by linear theory. Breaking occurs well below if $Hk \gg 1$.
- For more hydrostatic waves with $|m| \gtrsim |k|/\sqrt{2}$ waves break above the level predicted by linear theory. Breaking occurs well above if $|m/k|$ is large.

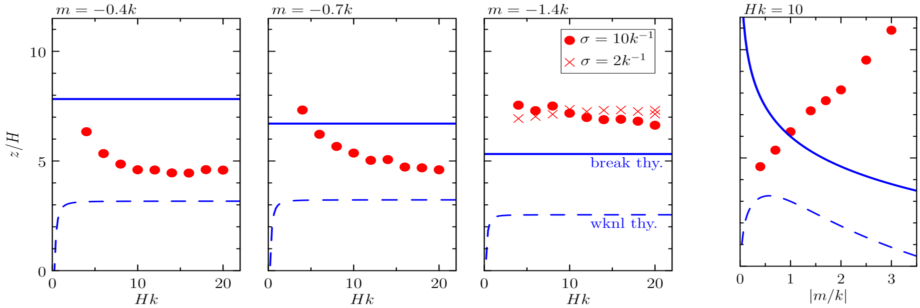

[Dosser & BRS, J. Atmos. Sci (2011)]

Simulated Overturning Heights

- Fully nonlinear 3D simulations are being performed to examine more precisely where momentum is deposited by a breaking anelastic wavepacket.
- Eventually the intent is to perform a wide range of simulations of wave breaking in realistic stratification and wind.
- Thus momentum transport may thus be included in GCMs using a look-up table.

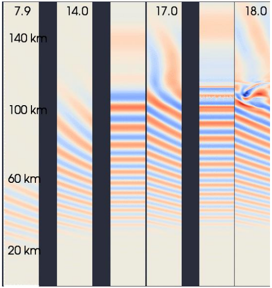

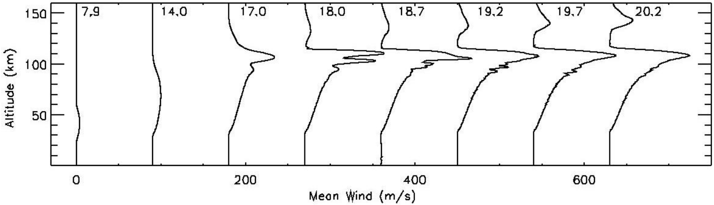

[Courtesy B. Laughman and T. Lund, Colorado Research Associates]

Summary and Outstanding Questions

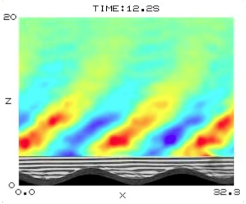

- Generation
  - Topographic generation (steady and tidal) is best studied.
  - Convection and turbulence also create waves.
  - *How important are non-topographic generation mechanisms?*

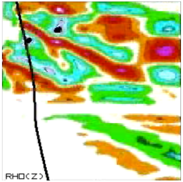

- Propagation
  - Ray (WKB) theory is used for waves in non-uniform media.
  - But this assumes their vertical scale is small compared to vertical background variations.
  - *Is WKB theory reasonably used to examine low mode internal waves?*

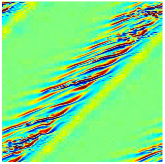

- Breaking
  - Waves evolve to breaking by approaching critical levels and are modified by weakly nonlinear modulations.
  - Ultimately they break down due to overturning, shear instability and PSI
  - *How do internal waves ultimately result in drag and mixing?*